Neural Networks 75 (2016) 56–65

Contents lists available at ScienceDirect

Neural Networks

journal homepage: www.elsevier.com/locate/neunet

Improved system identification using artificial neural networks and analysis of individual differences in responses of an identified neuron

Alicia Costalago Meruelo [a,*], David M. Simpson [a], Sandor M. Veres [b], Philip L. Newland [c]

[a] Institute of Sound and Vibration, University of Southampton, Southampton, UK
[b] Department of Autonomous Control and Systems Engineering, University of Sheffield, Sheffield, UK
[c] Centre for Biological Sciences, University of Southampton, Southampton, UK

ARTICLE INFO

Article history:
Received 30 April 2015
Received in revised form 3 October 2015
Accepted 4 December 2015
Available online 9 December 2015

Keywords:
Artificial neural network
Metaheuristic algorithm
Proprioception
Grasshopper
Motor neuron
Individual differences

ABSTRACT

Mathematical modelling is used routinely to understand the coding properties and dynamics of responses of neurons and neural networks. Here we analyse the effectiveness of Artificial Neural Networks (ANNs) as a modelling tool for motor neuron responses. We used ANNs to model the synaptic responses of an identified motor neuron, the fast extensor motor neuron, of the desert locust in response to displacement of a sensory organ, the femoral chordotonal organ, which monitors movements of the tibia relative to the femur of the leg. The aim of the study was threefold: first to determine the potential value of ANNs as tools to model and investigate neural networks, second to understand the generalisation properties of ANNs across individuals and to different input signals and third, to understand individual differences in responses of an identified neuron. A metaheuristic algorithm was developed to design the ANN architectures. The performance of the models generated by the ANNs was compared with those generated through previous mathematical models of the same neuron. The results suggest that ANNs are significantly better than LNL and Wiener models in predicting specific neural responses to Gaussian White Noise, but not significantly different when tested with sinusoidal inputs. They are also able to predict responses of the same neuron in different individuals irrespective of which animal was used to develop the model, although notable differences between some individuals were evident.

1. Introduction

Mathematical modelling has been used for many years to understand and describe biological systems, including their dynamics (Gamble & DiCaprio, 2003), the effects of experimental manipulation (Marder & Taylor, 2011), the impact of noise and variability (Sarkar, Christini, & Sobie, 2012) and how they change with ageing and disease (Horn, Ruppin, Usher, & Herrmann, 1993).

Linear and non-linear models, such as those derived by Wiener's method, have been widely used to quantify the behaviour of the nervous system (Kondoh, Okuma, & Newland, 1995; Marmarelis, 2004; Marmarelis & Naka, 1972). While these methods are powerful and provide quantitative descriptions of the linear dynamic transfer characteristics of a system (Marmarelis & Naka, 1973a) they can contain estimation errors due to background noise (Dewhirst, Angarita-Jaimes, Simpson, Allen, & Newland, 2012) and possibly overtraining of models (Tötterman & Toivonen, 2009). These estimation errors in turn produce erroneous predictions of the system's responses (Gamble & DiCaprio, 2003). Moreover, Wiener methods are not always applicable (Angarita-Jaimes et al., 2012) as the system expansion of the Wiener representation does not necessarily converge for all input functions (Palm & Poggio, 1977). In addition, such mathematical models have, in general, been fitted to the response to a stimulus of an individual (Dewhirst et al., 2012; DiCaprio, 2003; Marmarelis & Naka, 1972; Newland & Kondoh, 1997), without verifying if a particular model is a good representation of the population as a whole (Marder & Taylor, 2011). Using an average response to represent the population responses may be misleading due to different characteristics inherent to each individual (Goldman, Golowasch, Marder, & Abbott, 2001).

Recently, there has been an interest in modelling dynamic systems using Artificial Neural Networks (ANNs) since they have been found to model accurately many continuous functions (Haykin, 1999). In particular, they have been applied to chemical processes, plant identification and controller structures (Xing & Pham, 1995), and have been shown to have good predictive performance

* Correspondence to: SPCG, B13, University of Southampton, University Road, S017 1BJ, Southampton, UK.
E-mail address: acm1c08@soton.ac.uk (A. Costalago Meruelo).

http://dx.doi.org/10.1016/j.neunet.2015.12.002

in simulations of non-linear dynamic systems (Hunt, Sbarbaro, Zbikowski, & Gawthrop, 1992), financial markets (White, 1988), classification (Suraweera & Ranasinghe, 2008) and pattern recognition (Bishop, 1995). The choice of ANNs to model so many different systems is, in part, due to their flexibility, adaptability and generalisation capabilities (Benardos & Vosniakos, 2007) and their easy application in software and hardware devices (Hunt et al., 1992; Twickel, Büschges, & Pasemann, 2011). They have been applied successfully as robot locomotion controllers (Beer, Chiel, Quinn, Espenschied, & Larsson, 1992; Chiel, Beer, Quinn, & Espenschied, 1992; Cruse et al., 1995) by imitating the nervous systems that produce motion in insects' legs. Taken together these characteristics make them a powerful tool for non-linear model description and control system implementation.

The nervous system of insects, such as the desert locust, is relatively simple compared to mammals and a number of the constituent neurons with specific function are identifiable in different animals (Burrows, 1996) making them ideal to test the potential of ANNs to model neuronal responses, to analyse their generalisation abilities from one animal to the next and to understand individual differences in identified neurons. Imposed movement of the tibia, relative to the femur of the locust results in a resistance reflex that opposes the applied movement. This reflex can aid during stance and walking, in situations such as tripping or under the influence of other external forces (Field & Matheson, 1998). The Fast Extensor Tibiae (FETi) motor neuron, which is activated during reflex movements, is identifiable in every animal and has been studied for many decades and various mathematical models have been developed to understand its dynamics (Dewhirst et al., 2012; Dewhirst, Simpson, Allen, & Newland, 2009; Newland & Kondoh, 1997). The linear and non-linear properties of the FETi responses are well known, however, computational limitations in parameter estimation and the noise and variability of individual recordings have yet to be understood in detail (Angarita-Jaimes et al., 2012; Dewhirst et al., 2012). These challenges provide the motivation to test and validate ANNs as an effective mathematical method to model and describe the neural response across individuals.

The aim of this work was threefold: first to develop a method to design ANNs to model FETi responses and to determine whether they provide an improved performance over previous mathematical models; second, to understand the generalisation properties of the ANNs across individuals and to different input signals, and third, to understand individual differences in an identified neuron between individuals. To address these issues the performance of the ANN models was measured by their ability to predict responses of an individual as well as different individuals and their responses to different input stimuli.

2. Materials and methods

2.1. Data recording and post-processing

Adult male and female desert locusts (*Schistocerca gregaria*, Forskål) were mounted ventral surface uppermost in modelling clay and fixed firmly with one hind leg rotated through 90° and the femur–tibia angle set to 60° with the anterior face up. The apodeme of the femoral chordotonal organ (FeCO) was exposed by cutting a small window in the cuticle of the distal femur and grasped with a pair of forceps attached to a shaker (Ling Altec 101, LDS Test and Measurement) (Fig. 1). The apodeme was cut distally to avoid movement of the tibia thus opening the reflex-control loop. The thoracic ganglia were then exposed by removing the cuticle of the ventral thorax and also the air sacs and small trachea around the ganglia. A wax covered silver platform was then placed under the meta- and mesothoracic ganglia and the connectives cut posterior to the metathoracic ganglion. The ganglionic sheath

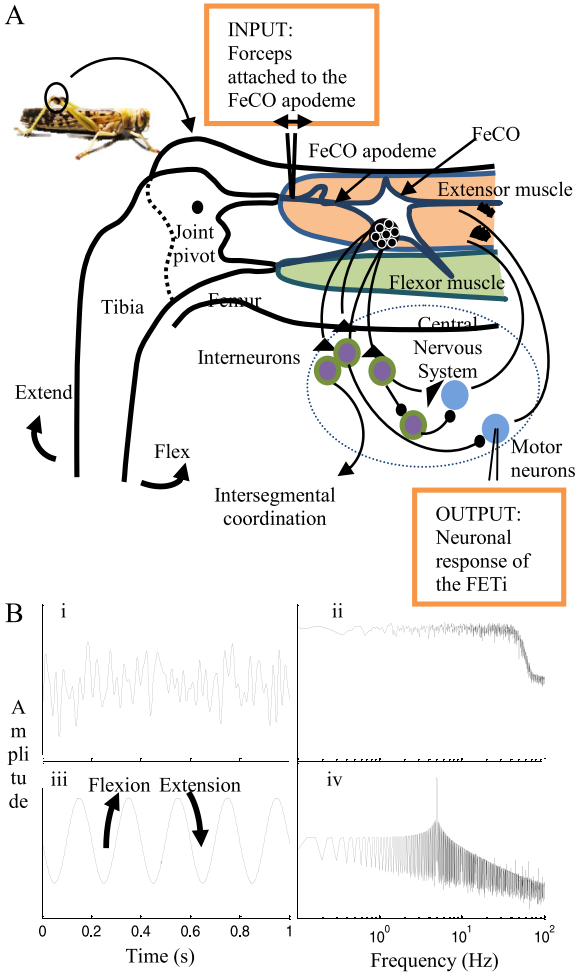

Fig. 1. (A) The components of the reflex control loop. The input was applied to the FeCO apodeme through a shaker and the output was the response of the FETi motor neuron. (B) The stimuli applied to the system included a band-limited Gaussian White Noise input shown in (i) the time domain and (ii) the frequency domain. A 5 Hz sinusoidal input was also applied and is shown in (iii) in time domain and (iv) in frequency domain.

was then softened by treating directly with protease (Sigma Type XIV) for 1 min (Newland & Kondoh, 1997). Intracellular recordings were made using glass microelectrodes, filled with 3M potassium acetate and with DC resistances of 50–80 MΩ, by driving an electrode through the sheath and into the soma of FETi. FETi receives monosynaptic and polysynaptic inputs from the femoral chordotonal organ (FeCO) that monitors movements of the tibia about the femur and which together underlie a simple resistance reflex that resists imposed movements of the hind leg (Field & Matheson, 1998).

The synaptic signals recorded in FETi were amplified and digitised with a sampling frequency of 10,000 Hz using a data acquisition board (USB 2527 data acquisition card, Measurement Computing, Norton, MA, USA) and stored for later analysis. They were then re-sampled at 500 Hz in Matlab® following a 3rd order low-pass anti-aliasing filter with a cut-off frequency of 250 Hz to remove residual high frequency noise (the spectrum of the recording is very low above 150 Hz). This re-sampling reduced the size of the files to process and, therefore, the computational time, without removing frequency components of interest. A high pass Butterworth filter of 3rd order and cut-off frequency of 0.2 Hz was applied to eliminate any slow time varying drift. A relatively small sample size of five was selected so that individual differences and similarities could be readily described, in addition to comparing

modelling methods. Since all the measurements from all animals were to be compared, and identical input signals were used in all animals, the responses were synchronised using cross-correlations between the input signals.

To move the chordotonal organ the shaker, on which the forceps grasping the apodeme of the FeCO was mounted, was driven with waveforms generated in MATLAB®, with a sampling frequency of 10,000 Hz. The displacements were applied to the apodeme via a digital-to-analogue (DA) converter (Fig. 1(C)) and included a Gaussian White Noise (GWN) (band limited to 0–50 Hz) and a sinusoidal (5 Hz) signal. The amplitude of the signals emulated the angular displacement of the tibia relative to the femur from 20°–100° approximately (Field & Burrows, 1982). We used GWN as an input to the system since it simultaneously excites all frequencies and amplitudes within a specified range and at thus reduces experimental and computational time. To test the ANN models with more realistic inputs, a sinusoid of 5 Hz was also applied to the FeCO (and later to the ANN) representing, approximately, the step frequency of gregarious locusts (Burns, 1973). The peak-to-peak displacement amplitude of the forceps was 1 mm, which represented the maximum linear displacement of the FeCO apodeme (Dewhirst et al., 2012; Field & Burrows, 1982). Previous studies have shown that the synaptic responses of FETi have a transient phase lasting approximately 3 s from the beginning of the FeCO stimulation, followed by a steady state period starting approximately after 10 s, with a transition period in-between (Dewhirst et al., 2012). Although ANNs are able to adapt during transient responses, to compare directly with previous methods, the signals used to train the networks were composed only of the steady state section of the responses (Dewhirst et al., 2012). All signals were visually inspected for the quality of the recording prior to analysis. The results are based on five successful recordings of 30 s duration of FETi responses to 50 Hz band-limited GWN inputs and 5 Hz sinusoidal inputs from five animals.

2.2. Artificial neural networks for system identification

We adopted a dynamical artificial neural network, based on a Feed Forward Neural Network (FFNN), known as a Time Delay Neural Network (TDNN) (Waibel, Hanazawa, Hinton, Shikano, & Lang, 1989), to model FETi responses. This type of network uses delayed versions of the input to estimate the output, which turns a static FFNN into a dynamic network (Haykin, 1999), assuming that the response of FETi was a combination of the current and past input samples. The architecture of the ANN was formed by an input and an output layer and a series of hidden layers, each of which was formed by a determined number of nodes. A node is defined mathematically as follows:

$$y = f(\Sigma_i w_{ji} x_i + \theta_i) \tag{1}$$

where x and y are the i inputs and outputs respectively of the jth node, w_{ji} are the weights for each input, θ_i is the bias and $f(x)$ is referred to as the activation function (Xing & Pham, 1995).
The activation function $f(x)$ (Eq. (2)) used in the hidden layers of both networks is a sigmoid function, the most used activation function (Jain, Jianchang, & Mohiuddin, 1996; Xing & Pham, 1995).

$$f(x) = 1/(1 + e^{-x}). \tag{2}$$

This function was used to introduce a non-linearity in the estimated output. The output layer also contained a node, whose transfer function was a linear function instead of a sigmoid function, meaning that all the non-linear calculations occurred within the hidden layers.

The Matlab® `timedelaynet` built-in function was used to design the ANN network, specifying the number of layers and delays and the training function. A Levenberg–Marquardt back-propagation algorithm was used for training the network and to calculate the weights between nodes. This algorithm is a version of the back-propagation algorithm, chosen for its accuracy and fast convergence compared to classical back-propagation algorithms (Bishop, 1995; Webb, Lowe, & Bedworth, 1988). The number of samples in the input vector (i.e. the delayed input signal) was set to 100 samples (corresponding to an impulse response of 0.2 s in duration), based on preliminary optimisation studies. This value is similar to the length of the impulse response for the LNL model applied to the same data (120 samples, Dewhirst et al., 2012). Each time the network is trained, its performance depends on the initial value of the weights (which are usually initialised randomly). To remove this additional source of variation between individuals, the initial weight values were specified in the network description and the same set of initial values was used for each network.

2.3. Metaheuristic algorithms for ANN architecture design

The performance of ANNs depends greatly on the number of nodes and layers of the ANN chosen. In this work we used a metaheuristic algorithm to indicate an optimal architecture. The algorithm was a combination of two metaheuristic algorithms: Evolutionary Programming (EP) (Eiben & Smith, 2003) and Particle Swarm Optimisation (PSO) (Kennedy & Eberhart, 1995). The algorithm combined the characteristics from metaheuristic optimisation methods proposed in the literature (Angeline, Saunders, & Pollack, 1994; Benardos & Vosniakos, 2007; Suraweera & Ranasinghe, 2008).

The algorithm is composed by a series of functions (Fig. 2). The first function of the algorithm creates a population of potential ANN's with individuals having specific architectures with up to 5 hidden layers and 32 nodes in each layer.

$$x_\eta = [n_1\ n_2\ n_3\ n_4\ n_5] \tag{3}$$

where x_η is a vector representing an individual's architecture, η is the specific individual within the population, and n_i are the number of nodes in each of the five layers of the ANN. The number of nodes in each layer was modified at every generation through variation operators, until an optimal solution was found. The optimal architecture was a trade-off between the performance of the network and its complexity (total number of nodes), with the performance being defined here as the prediction accuracy, while the complexity is defined by its size (i.e. the number of hidden layers and nodes). Once each individual from a population had been randomly initialised, the population 'evolved' over a number of generations.

The algorithm contains a series of functions used in the generation of each ANN (Fig. 2). The first function was a cleaning function designed to avoid empty ANNs during the iteration process, i.e. networks that had no nodes in any layer, and were thus formed by just an input and an output. When the population was created and passed through the cleaning function, the networks were trained with the 50 Hz band-limited GWN response of FETi. The training signal was composed of two thirds of a recording of FETi from either one individual animal or the averaged response from all five animals. The training data (2/3 of the recording) was then divided into another three sections to use in the training process, one for training the weights (70%), one for validating them (15%) and one for testing its response (15%). The validation data is used during the calculation of the weights to check whether the network is improving and the testing data is used at the end of the training process to check whether the training has been successful.

To determine how close to the optimal solution the networks were, their fitness was calculated on the remaining third of the recording, not used with the training algorithm. The optimal

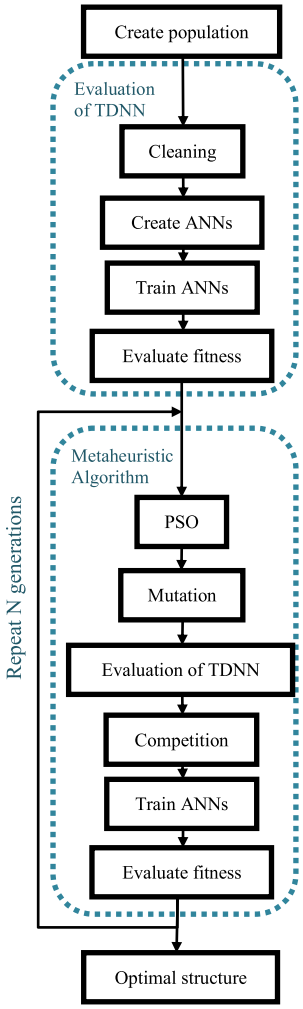

Fig. 2. Flow chart of the algorithm used to design the architecture of the feed-forward network combining the metaheuristic methods of Evolutionary Programming (EP) and Particle Swarm Optimisation (PSO). This algorithm was repeated either for a number of specified generations or until it converged, with every member of the population having the same unchanging architecture.

performance was represented by the highest fitness in the search space, which was a combination of two traits: high performance and low complexity. To estimate the performance, the Normalised Mean Square Error (NMSE) was calculated (Eq. (4)), between the estimated output and the recorded output.

$$\text{NMSE}(\%) = 100\left(\sum_{i=1}^{N}(y_i - \hat{y}_i)^2\right) / \left(\sum_{i=1}^{N}(y_i)^2\right) \tag{4}$$

where y_i is the measured output in the FETi at the ith sample and $\hat{y}_i$ is the estimated output of $\boldsymbol{N}$ samples, from the trained neural network.

The fitness function designed (Eq. (5)) seeks a compromise between the goodness-of-fit of the network and its complexity and is based on that used by Benardos and Vosniakos (2007).

$$fit = e^{(100/\text{NMSE}(\eta) - a \cdot n(\eta))} \tag{5}$$

where NMSE is the Normalised MSE (%) as described in Eq. (4) of the individual η, and $n(\eta)$ is the total number of hidden neurons of the individual network η. a is an adjustable parameter set in this case to $a = 0.002$, which relates the importance of the size to the accuracy of the network. This value was chosen through trial and error methods, where high performances and small size networks were rewarded. Although the computational time is not directly taken into account in the fitness function, the networks are set to train for only 200 epochs (iterations of the back-propagation algorithm), and therefore those that had not converged, and needed a longer time to train, would result in a higher NMSE value and the faster ones would show higher fitness.

Once the networks had its fitness calculated, variation operators were applied to the population that were defined by the evolutionary algorithms (first PSO and then EP) and the fitness function. First, PSO was applied. The global and individual best ANNs were found to use with the PSO equations (Shi & Eberhart, 1998a), and the 'velocity' of each individual calculated (Eqs. (6a) and (6b)). The architecture of the individual represents its position (a vector of five parameters that represent the number of nodes in each layer), and the velocity of the individual is the change in the number of nodes in the architecture between the past iteration and the current iteration, is represented as another vector with five parameters. The global best was the architecture with the highest fitness obtained so far over the generations throughout the whole population. The individual best was the best performing architecture obtained by each individual over the generations. In each of the generations, the individuals were 'moved' with a certain 'velocity' towards the best performing architectures in the search space, namely those with highest fitness, according to the equation below.

$$v_\eta(t+1) = i v_\eta(t) + 2R_1(p_\eta - x_\eta(t)) + 2R_2(p_g - x_\eta(t)) \tag{6a}$$

$$x_\eta(t+1) = x_\eta(t) + v_\eta(t+1) \tag{6b}$$

where η is the individual, v_η is the velocity of the individual at generation t, i is the inertia weight, p_η is the personal best position of the individual, x_η is the actual position (i.e. number of hidden layers and nodes in each layer of the individual, as in Eq. (3)), p_g is the global best position of the population and R_1 and R_2 are random numbers in the range [0, 1]. Using these 'velocities' (Eq. (6a)) the population is 'moved' towards those architectures that progressively represent the measured system better. The inertia weight i was set to 1.05 for this case, since it has been suggested that values between 0.8 and 1.2 are those that give the algorithm the best chance of finding the global optimum (Angeline et al., 1994; Shi & Eberhart, 1998a). The value 1.05 was selected for its ability of finding the optimal value without failures (Shi & Eberhart, 1998a, 1998b).

Once the population was moved towards the global and personal best through PSO, it was mutated using EP. The mutation rate of the algorithm is a dynamic rate based on the evolutionary algorithm of Angeline et al. (1994), dependent on the fitness of the individuals (Eq. (7)). The purpose of the dynamic mutation rate is to encourage big changes for those individuals with poor performance and a fine tune search when the networks are near the optimum. Instead of using the maximum fitness achievable which is unknown, the fitness of the global best individual is used, and results in the global best architecture not being mutated in that generation.

$$R = 1 - \text{fit}(\eta)/\text{fit}_{\max} \tag{7}$$

where $fit(\eta)$ is the fitness of the individual and $fit_{\max}$ is the fitness of the currently global best architecture.

To ensure that only the architectures with higher fitness are transmitted to the next generation, a competition function is included. This function compares the fitness of each couple of parent and offspring, retaining in the next generation the one with the higher fitness, assuring the survival of the fittest.

The optimisation process was repeated over a number of iterations, or generations, and the output of the algorithm was considered to be the optimal architecture and used to predict the data recorded from the FETi motor neuron.

Table 1
The architectures of the ANNs obtained for FETi in 5 different animals. Each network is composed of two hidden layers of up to 8 neurons in each.

	Layer 1	Layer 2
Animal 1	6	1
Animal 2	4	1
Animal 3	6	2
Animal 4	8	7
Animal 5	8	3
Average response	**5**	**2**

2.4. Linear Nonlinear Linear (LNL) model

The Linear–Nonlinear–Linear model, also known as Wiener Hammerstein model (Hunter & Korenberg, 1986), is a cascade model consisting of two dynamical linear elements separated by a static nonlinear element, of the form:

$$y(t) = \sum_{\sigma=0}^{T-1} g(\sigma) \sum_{q=0}^{Q} C^{(q)} \left(\sum_{\tau=0}^{T-1} h(\tau) u(t-\sigma-\tau) \right)^{q} \quad (8)$$

where $g(\sigma)$ and $h(\tau)$ are the dynamic linear elements, $C^{(q)}$ represents the coefficients, u is the input and y the output.

This model is a subset of the Volterra series. The coefficients of the model can be calculated using different optimisation methods, such as the Least Squares method or a method developed by Korenberg and Hunter (1986) based on the Levenberg–Marquardt algorithm.

To compare the responses produced by the ANNs, the results from the LNL models developed by Dewhirst et al. (2012) are used, since they have been designed using the same recordings.

3. Results

3.1. FETi responses to FeCO apodeme displacement

Displacement of the apodeme of the FeCO evoked a synaptic response in FETi. Stretches of the apodeme, equivalent to flexions of the tibia, evoked depolarisations, whereas relaxation of the apodeme, equivalent to extensions of the tibia resulted in hyperpolarisation, typical of a resistance reflex (Fig. 3(A)) (Field & Matheson, 1998). The responses of FETi to displacement of the FeCO apodeme with a 50 Hz GWN stimulus resulted in the synaptic responses following, approximately, the input signal (Fig. 3(B)). The responses of FETi to the same stimulus input in different animals ($n = 5$) appeared similar although there was some clear variability, or individual differences, between animals (Fig. 3(C)).

To estimate a representative response of FETi across all individuals, an average response was calculated from the recorded FETi signals from 5 animals (shown in Fig. 3(B)). This average response was later used to determine whether it can be considered representative of the system. It was also used to study the inter-animal variability of the FETi motor neuron response and the ANN model generalisation.

3.2. Architectures of the ANN models

The metaheuristic algorithm was run once for each FETi response and once for the average, a total of six times, over 50 generations. The output of the algorithm provided the architectures of the ANNs used to model each of the individual responses and were composed of up to two hidden layers, with each layer with between one and six nodes (Table 1).

The architectures for the individual responses and the average response were similar, although the algorithm allowed for networks with up to 32 neurons and 5 hidden layers. All networks were relatively small (Table 1) and were composed of two hidden layers with between 1 and 8 nodes in each layer.

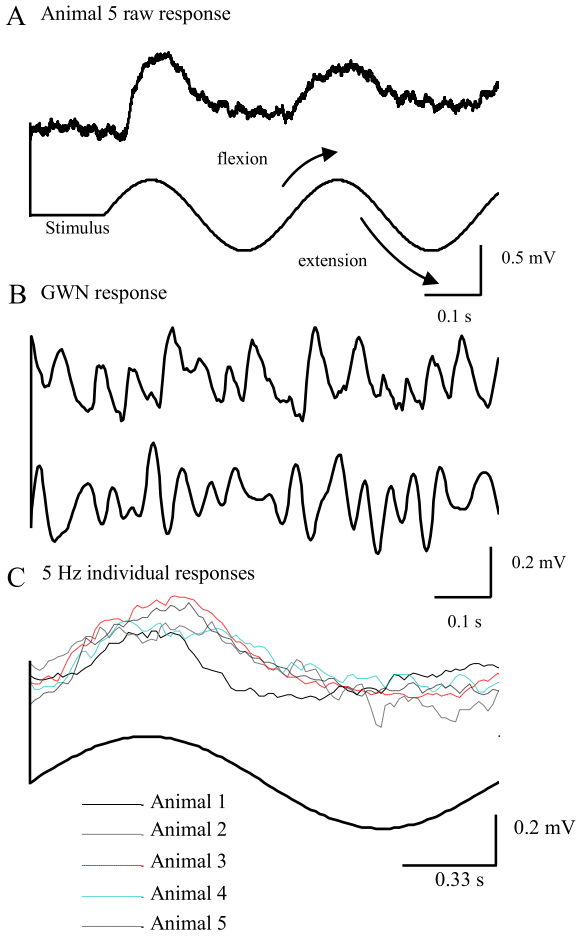

Fig. 3. Response of the FETi motor neuron to a 50 Hz band-limited GWN stimulus and a 5 Hz sinusoidal stimulus applied to the FeCO apodeme. (A) Raw response to 5 Hz before post-processing, including background noise and the stimulus onset. (B) Average GWN response after post processing. (C) Responses of FETi from 5 different animals to a 5 Hz sinusoidal stimulus.

3.3. Validation of the ANNs

The architectures obtained with the metaheuristic algorithm were trained for each of the FETi responses obtained from different animals (Fig. 3) using GWN as an input signal. An individual model, such as that for Animal 5 (Fig. 4(A)), was able to follow the response to the GWN signal quite well. The models for individual FETi responses from the different animals had a range of performance when tested with previously unseen data (the 1/3 of data not used in the network training) from the same individual. The model of FETi in Animal 3 had the best performance, with a NMSE of 15.5% (Table 2), indicating that the model was able to predict well, most of the FETi response. The models performed less well in other animals, with NMSEs of 29.4% in Animal 1, 18.1% in Animal 2 and 16.9% in Animal 5. The model for Animal 4 was the worst performing, with a NMSE of 33.7%. Together, these models produced an average NMSE of 21.6 $\pm$ 7.9% (NMSE $\pm$ Standard Deviation, SD), which represents the prediction error on unseen data from the each of the responses.

An ANN optimised for the average response also produced a good performing model with 5 nodes in the first hidden layer and 2 in the second (Table 1). This model had a NMSE of 15.8% (Fig. 4(B)), slightly worse than that of the best performance seen using individual responses of FETi from different animals, but better than any other model. This improved performance may be expected since the averaging process reduces the additive noise in the recordings.

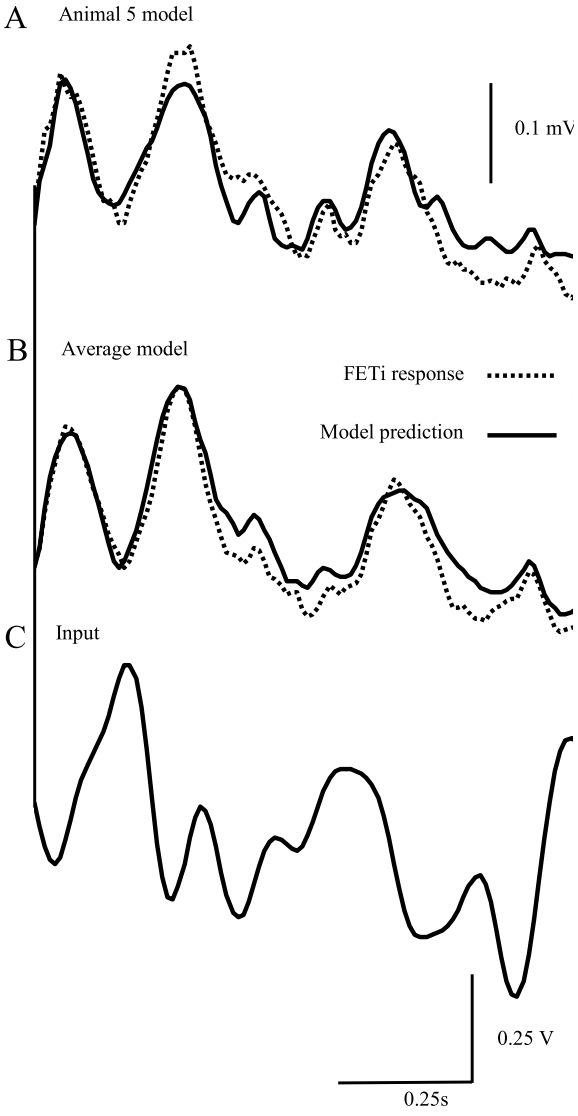

Fig. 4. ANN fit to Animal 5 and the average response. (A) The networks have been trained with two thirds of the FETi motor neuron response from Animal 5 to 50 Hz band-limited GWN. (B) Network trained with two thirds of the average response to 50 Hz band-limited GWN. (C) Input GWN signal applied to the system.

Table 2
NMSE (%) of the performances of the TDNN and LNL (from Dewhirst (2013)—using the same procedure on the same data) for GWN and the 5 Hz sine-wave.

Model	TDNN		LNL	
Testing signal	GWN	5 Hz	GWN	5 Hz
Average response	15.8	8.4	36.9	13.4
Animal 1	29.4	39.4	32.1	13.4
Animal 2	18.1	40.0	27.5	16.3
Animal 3	15.5	9.0	30.7	44.9
Animal 4	33.7	26.5	41.2	82.9
Animal 5	16.9	14.2	27.8	33.3
Mean	*21.6*	*22.9*	*32.7*	*34.1*

The performance of all the individual ANNs, expressed as NMSE, was compared to the Linear–Nonlinear–Linear (LNL) model designed by Dewhirst et al. (2012). Both models behaved similarly (Fig. 5), although the TDNN models consistently had lower prediction errors. The TDNN had a mean NMSE of 21.6% while the LNL models had a mean NMSE of 27.5%. A Mann–Whitney U test, chosen for the small sample size and the non-normality of the data, showed that the performances between the TDNN and the LNL

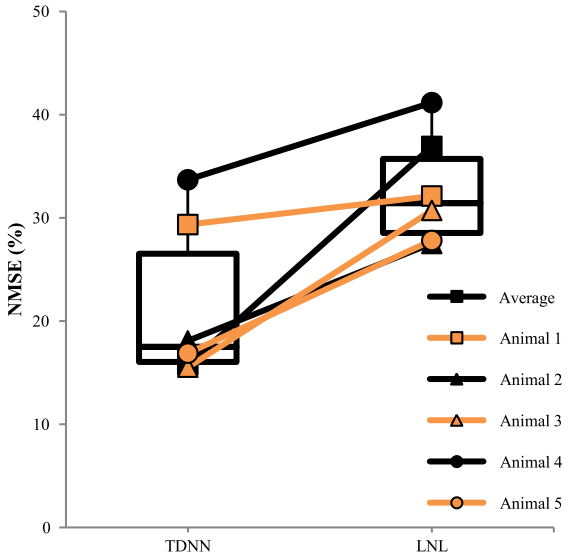

Fig. 5. Comparison of the NMSE of the TDNN and the LNL cascade models. The NMSE of the models was calculated when training and testing the models with 50 Hz band-limited GWN. Testing was carried out on data not used in training, but from the same individual. The NMSE was bigger for the LNL model in all individuals. The box-plots represent the median and quartiles and the whiskers extreme values of the same data.

were significantly different ($U = 6.0$, $p = 0.05$), which suggests that the ANNs were better at predicting FETi responses to GWN.

3.4. Validating ANNs with sinusoidal inputs

To validate the ANN models estimated from a GWN input signal, their ability to predict a FETi response to 5 Hz sinusoidal stimulus applied to the FeCO was determined. An individual model, such as the model optimised for Animal 5 and trained with GWN predicted approximately the 5 Hz response from the same individual (Fig. 6(A)). The NMSE from individual responses ranged from 9.0% to 40.0% (Table 2). The best performing animal with GWN (NMSE of 15.5%) was also the best performing animal with a 5 Hz sinusoidal input (Animal 3 with NMSE = 9.0%). The worst performing animal with GWN (Animal 4), however, was not the worst performing with 5 Hz sinusoidal input (Animal 2 with NMSE = 40.0%). The performance of the TDNN trained with the average response and tested with a 5 Hz sinusoid had an NMSE of 8.4% (Fig. 6) showing that the GWN-trained ANN model was able to predict more than 91% of the responses to the sinusoidal input signal. The previous LNL models described by Dewhirst et al. (2012), when tested with 5 Hz sinusoidal inputs, showed a performance ranging from NMSE of 15% to 83%. A Mann–Whitney U test showed that while the means appear very different, the performances with 5 Hz input of the TDNN (with mean NMSE = 22.9%) and the LNL (with mean NMSE = 34.1%) were not significantly different ($U = 13.0$, $p = 0.49$), due in part to the considerable variability of both the ANN and the LNL models with different individuals (TDNN has considerably lower NMSE in only three of the five animals), and the small sample size. The ANNs can thus be considered at least as accurate, if not better, than LNL and Wiener methods (Dewhirst et al., 2012) at predicting unseen sinusoidal data from FETi recordings.

3.5. Generalisation of the ANNs to FETi responses in different animals

The FETi responses from different animals showed clear individual differences, or variability (Fig. 3). Understanding the underlying common responses of the same neuron between

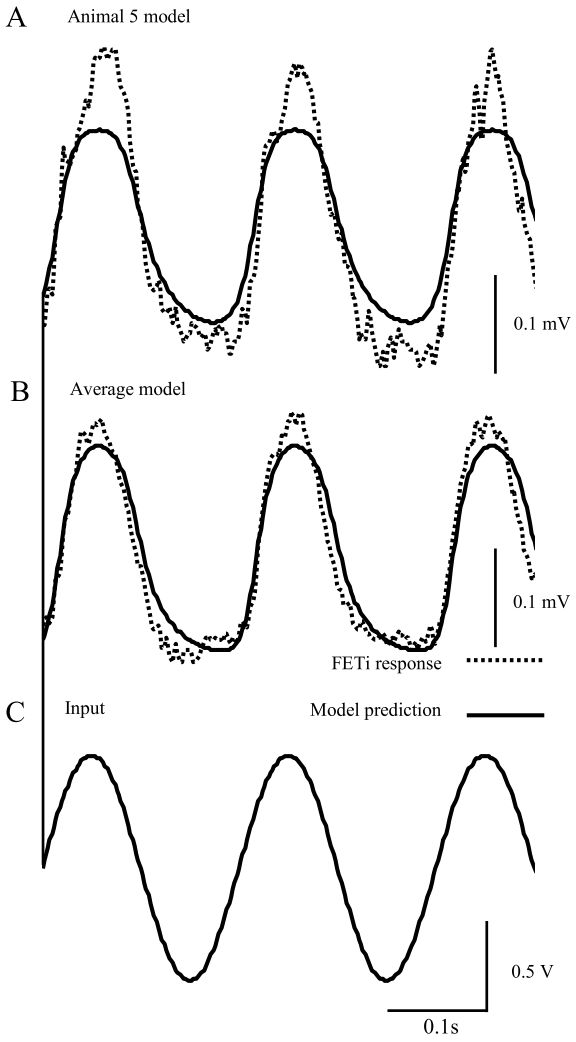

Fig. 6. Generalisation of the TDNN when trained with GWN and tested with a 5 Hz sinusoid. (A) Measured signal in Animal 5, and its prediction from the individual model optimised with GWN prediction. (B) Average signal and its prediction from the ANN model optimised on GWN stimuli and the averaged responses. (C) Input signal to the FeCO.

individuals and where the differences between individuals lie, could aid in a better understanding of how nervous systems generate behaviour. We therefore asked how accurately a model designed for one particular individual can predict the response from another individual. For this purpose, the ANNs trained with individual responses were tested with all the animal responses and their NMSE calculated (Fig. 7).

The performances of the ANNs showed an average NMSE of 47.7% (SD = 32.4%) for all tests. This indicates that any of the ANNs designed can predict on average 52.3% of the response in any individual FETi in different animals. The ANN trained with the average response had a lower NMSE when predicting the individual responses, with an average NMSE 34.2% (SD = 23.9%). A network trained with the average response could predict therefore an average of 65.8% of the responses in any individual.

To test whether there was a difference in the generalisation power of the models based on the training signal used, a Friedman test was applied. The test, run across the NMSEs from all models, was not significant ($\chi^2 = 8.93$, $p = 0.063$). Therefore, no individual model was significantly better or worse than any other in generalising to other animals.

Although most of the individual responses were similar, all models fail to predict the synaptic responses from Animal 4,

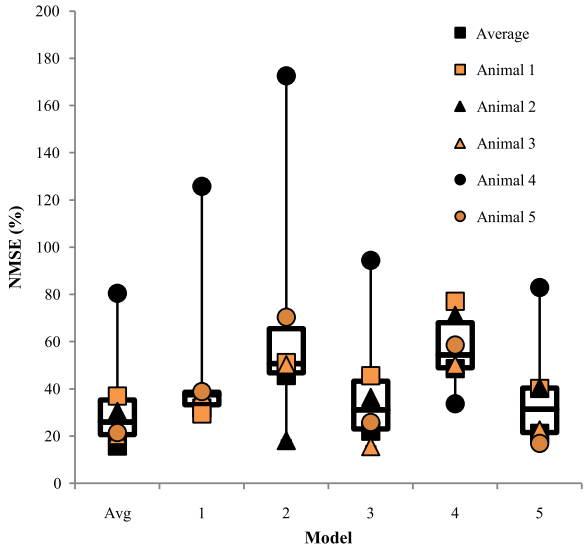

Fig. 7. NMSEs of all the ANN models to predict recordings from each of the other animal and the averaged response. The abscissa refers to the signal used in training and each symbol reflects the signal used in testing. The NMSE value was calculated after the networks were trained with 50 Hz band-limited GWN and tested with unseen 50 Hz band-limited GWN. The box-plots represent the median and the quartiles and the whiskers extreme values of the data. Each individual value is also shown. Results showed that no specific model was the best performing model and statistical tests indicate that there were no significant differences between model performances (Friedman's test, $p > 0.05$).

excluding the ANN trained with data from Animal 4 (black circles in Fig. 7). This may be considered an illustration of inter-subject variability of the FETi responses, where Animal 4 appears to behave differently from other individuals. Considering that not all the FETi responses can be predicted perfectly with any model, other factors might be present that influence the output and are not taken into account in the modelling process.

3.6. Variability between individuals

In the previous section we focused on the six models estimated and asked how well each could predict the FETi responses. The counterpart to this question is addressed now, by focusing on each recording, and asking how well they are predicted by any of the models.

As seen in Fig. 8, Animal 3 and the average response to GWN were the best-predicted responses by all the individual models, with an average NMSE of 32.73% (SD = 15.4%) and 30.83% (SD = 13.7%) respectively. Animal 4 was the worst predicted individual response by any model (as already observed above), with an average NMSE of 98.3% (SD = 46.9%). A Friedman test was conducted to determine whether there was a difference for an individual response to be predicted by any model, i.e. the inter-subject variability. The test showed that the individuals were significantly different from each other when being predicted by any ANN model ($\chi^2 = 11.5$, $p = 0.04$). A Wilcoxon signed-rank test with a Bonferroni correction (significance level of $p < 0.003$) showed that the individuals, grouped by pairs, were not significantly different from each other ($p > 0.046$).

4. Discussion

The results of this study indicate that ANNs can be used to model responses of individual neurons in neural networks and can be used to explore and understand individual differences in their responses.

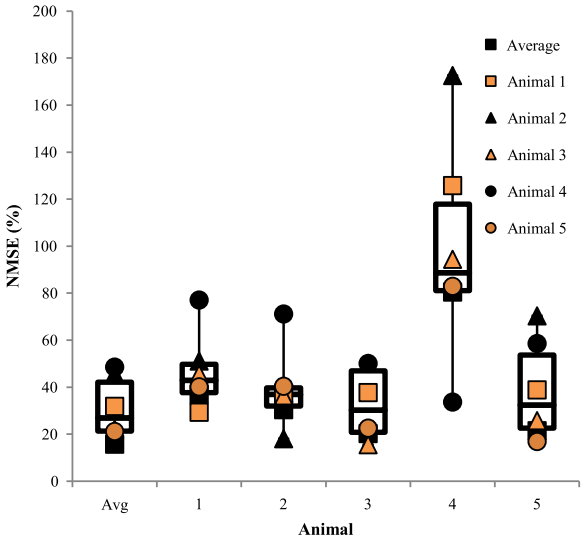

Fig. 8. NMSEs of all the animals when predicted by each of the ANN models. The abscissa refers to the animal used in testing and each symbol reflects the animal used in the model training. The box-plots represent the median and the quartiles and the whiskers extreme values of the data. The figure is based on same data as used in Fig. 7, but presented ordered by animal, rather than by model. The model from Animal 4 clearly provided the worst prediction, except in predicting the response of Animal 4. Statistical results showed that there were no significant differences between individuals (Friedman, $p > 0.05$).

We have developed a method to design architectures for ANNs to model the synaptic responses of an identified motor neuron in a proprioceptive neural network. The metaheuristic algorithms optimised the ANN architectures to reduce computational time and improve their generalisation abilities. The ANNs were more accurate at predicting GWN responses in FETi than previously tested methods on the same neuron (Dewhirst et al., 2009). However, the ANNs were not significantly better at predicting the response to the sinusoidal input than the previously used methods (Dewhirst et al., 2009; Dewhirst et al., 2012; Newland & Kondoh, 1997).

We have shown, for the first time, that the models developed from a specific individual neuron can generalise well and predict the responses of the same neuron in other animals. This suggests that an ANN model could be used as a mathematical representation of the FETi neuron response to FeCO stimulation in any locust based on system estimates from one individual, with the caveat that predictions tend to be better when the same individual is used in training the model. This points to some individual differences and in our sample of five locusts, four were similar, but one (Animal 4) was clearly more distinct. There are a number of possible reasons for why the model fit is not perfect, even within each individual: there may be some adaptation (variation over time) in the response over the duration of stimulation; the low complexity of the models may not allow subtle features of the responses to be captured; additional inputs to the FETi not taken into account in the model; noise due to the electronic recording system. Perhaps the main contributor is spontaneous neuronal activity (noted even before stimulation commences) (Burrows, Laurent, & Field, 1988) and no input–output model would be able to account for that. In the current approach, all these factors would be captured in the mean-square error and contribute to the NMSE.

4.1. Comparison with other modelling methods

The results suggest that ANNs can be used as mathematical tools to study neural responses with a high degree of accuracy. Moreover, they have been shown to outperform previous LNL and Volterra methods ((Dewhirst, 2013; Dewhirst et al., 2009; Newland & Kondoh, 1997)) in predicting the responses of FETi to a GWN displacement of the FeCO apodeme, with an approximate improvement of 10% over LNL methods (Dewhirst, 2013) and a 25% improvement over Wiener methods (Newland & Kondoh, 1997). Both ANN and LNL methods have also been shown to be able to predict sinusoidal responses, where the model used was trained with 50 Hz band-limited GWN data from the same individual in which the synaptic responses of FETi to 5 Hz sinusoidal stimulation were recorded. The mean square error of the TDNN method was much lower than that obtained with Wiener methods (Dewhirst, 2013) but was not significantly different from LNL methods. This suggests that the ANNs and LNLs were similarly good at predicting responses to different inputs within the same animal. The small sample size together with considerable individual variability in the NMSE contributed to this result; clearly ANN is not better in every individual.

Other studies have also used Wiener methods to model neural responses to GWN stimuli. For example, Marmarelis and Naka (1973b) modelled the averaged intracellular responses of neurons in the catfish retina using Wiener kernels, with a NMSE of 25% or less, using modulated light as the white noise input stimulus. Proprioceptors in a chordotonal organ in the crab were also modelled using Wiener kernel methods (DiCaprio, 2003) and the NMSE of the second-order models was around 6%–26% when tested with data from the same individual. The NMSE obtained with ANNs in FETi in the current work is comparable to that obtained using Wiener models of the same neuron, but is not as accurate as other Wiener methods applied in other neuronal systems. The most likely explanation of which is that the studies by DiCaprio (2003) on the crab and Marmarelis and Naka (1973b) on the catfish focused on the input stages to the neural networks, whereas here we focused on the output, a motor neuron, FETi. The consequence of this is that FETi responses not only include those correlated with the stimulus input but also uncorrelated spontaneous synaptic responses typical of central neurons that clearly cannot be predicted from the input signal (see for example Burrows, 1987; Büschges, Kittmann, & Schmitz, 1994; Field & Burrows, 1982).

The advantage of using ANNs however, is that not only can they predict accurately the responses to an input, but they are also able to predict responses to other inputs and, furthermore, able to predict responses in different individuals using the same model. Such modelling technique provides the flexibility that any animal could be used to train the networks, namely an individual response to a stimulus or even the average response calculated across different individuals.

One should add that the comparison between models also depends on how the model order was chosen, and the conclusion that one model is 'better' than another has to be considered with some caution, especially when the performance does not differ by very much and there are quite large differences in performance in different individual animals.

4.2. Variability across individuals

Goldman et al. (2001) and Marder and Taylor (2011) suggested that models based on individual or averaged responses may not be representative of the system across a population of individuals due to variability and individual differences even within identified neurons. A mathematical model able to capture the common response in different individuals would be able to describe better the responses within the population. However, as far as we know, no generic mathematical model of neural responses in identified neurons has been tested across different individual responses. Our results show that the individual responses of FETi can be predicted by any of the ANN models developed from FETi in any other

animal, although usually with higher NMSE, independently of the data used to train the network. The model fitted to the averaged responses tended to give a better fit across all individuals (see Fig. 8), but this was not consistently observed.

Using the performances of the models, it has also been shown that the individual responses are not significantly different from one another. Previous studies have shown that mathematical models of FETi (Dewhirst et al., 2009; Newland & Kondoh, 1997) produced similar values of NMSE when the model was developed and tested with data from the same individual. Such models, however, were never used to test their applicability to the responses of other individuals. DiCaprio (2003) and Marmarelis and Naka (1973b) also used Wiener methods, but again did not test their applicability across individuals. It is notoriously difficult to interpret ANN models behaviour, and applying the models between individuals provides a means of assessing their similarity. The conclusion that models fit well between individuals suggests that results from one individual, or a small sample of individuals, provide a good approximation to the behaviour of the identified neurone *per se*.

The errors observed in the ANN models when tested with different individual responses can only partly be explained by differences across animals as a result of spontaneous activity found in central interneurons and motor neurons (Büschges, 1990; Field & Burrows, 1982). The observation that performance is consistently best when the model is trained on the same individual from which the (previously unseen) test data is taken, suggests that the models are distinct, not just that the noise levels differ. Variability has been shown in the synaptic properties of identified neurons, where responses across individuals differ, while the overall neural circuit behaviour remains the same, or similar, in all individuals (Marder & Taylor, 2011). Another explanation for these differences is small variations in the encoding of a stimulus in each individual. Schneidman, Brenner, Tishby, van Steveninck, and Bialek (2001) showed that approximately 30% of the information in an identified motor neuron in flies is specific to each individual, whereas the remaining 70% is a common response which is similar in the same motor neuron from the whole population of flies. Such a common response might also be present in the FETi, where the ability of the ANNs to predict part of the responses in all individuals represents a common response to all in the population, whereas the individuality of the responses, or uncorrelated spontaneous activity, remains as errors.

Nonetheless, the errors in the responses might not be entirely due to inherent differences between animals, but also may include differences within the same animal, such as variations over time, or across individuals, such as small changes in experimental methods (i.e. precise location of the electrodes). The nature of the experiments is such that repetition (with renewed insertion of electrodes) is not practicable.

Whether the average response is the most appropriate characteristic to represent a system is still debatable (Goldman et al., 2001; Marder & Taylor, 2011). Our results suggest that an ANN model fitted to the responses averaged across individuals, provides a fairly good fit in all animals, and may thus be deemed as representative. The models developed were able to predict responses in different individuals, which show that FETi responses share common features across different individuals, but the responses contain some individuality that cannot be predicted by a generic model. Caution is recommended in assuming any model represents the behaviour of the identified neurone across a population.

In summary, the ANN models designed in this study have been shown to be significantly better than previously explored mathematical models of the FETi responses to GWN. ANNs thus provide a promising method in the study of the neural responses and similarly structured networks in locust and other species. The average response provides a robust basis for model fit, although further evidence of the presence of individual differences was found. The models designed with ANNs thus appear promising as a tool in analysing neuronal reflexes and may guide the future design of engineering control systems or medical assistive devices.

4.3. Conclusion

Here we show that ANNs can be used to model the synaptic responses of an identified motor neuron in a proprioceptive neural network to a GWN stimulus with more accuracy than previously used methods, such as Wiener or LNL models, and with undistinguishable accuracy following sinusoidal stimuli. We have developed a new method to optimise the ANN architecture, which reduces computational time and improves the generalisation abilities of the networks. ANNs thus appear promising tools for the analysis of neuronal networks. We show that ANN models are able to predict responses to other (previously unseen) inputs and, furthermore, the responses of the same motor neuron in other animals. Any ANN model was able to estimate the responses in any individual, although predictions tended to be better within the same animal, highlighting the common function of the motor neuron in different animals, as well as some individual differences.

Acknowledgements

Alicia Costalago Meruelo was supported by an EPRSC grant (EP/G03690X/1) from The Institute of Sound and Vibration Research and the Institute for Complex Systems Simulations at the University of Southampton. Data supporting this study are openly available from the University of Southampton repository at http://dx.doi.org/10.5258/SOTON/385038.

References

Angarita-Jaimes, N., Dewhirst, O. P., Simpson, D. M., Kondoh, Y., Allen, R., & Newland, P. L. (2012). The dynamics of analogue signalling in local networks controlling limb movement. *European Journal of Neuroscience*, *36*(9), 3269–3282.

Angeline, P. J., Saunders, G. M., & Pollack, J. B. (1994). An evolutionary algorithm that constructs recurrent neural networks. *IEEE Transactions on Neural Networks*, *5*(1), 54–65.

Beer, R. D., Chiel, H. J., Quinn, R. D., Espenschied, K. S., & Larsson, P. (1992). A distributed neural network architecture for hexapod robot locomotion. *Neural Computation*, *4*(3), 356–365.

Benardos, P. G., & Vosniakos, G.-C. (2007). Optimizing feedforward artificial neural network architecture. *Engineering Applications of Artificial Intelligence*, *20*(3), 365–382.

Bishop, C. M. (1995). *Neural networks for pattern recognition*. New York, NY, USA: Oxford University Press.

Burns, M. D. (1973). The control of walking in orthoptera. *Journal of Fish Biology*, *58*(1), 45–58.

Burrows, M. (1987). Parallel processing of proprioceptive signals by spiking local interneurons and motor neurons in the locust. *The Journal of Neuroscience*, *7*(4), 1064–1080.

Burrows, M. (1996). *The neurobiology of an insect brain*. Oxford: Oxford University Press.

Burrows, M., Laurent, G. J., & Field, L. H. (1988). Proprioceptive inputs to nonspiking local interneurons contribute to local reflexes of a locust hindleg. *The Journal of Neuroscience*, *8*(8), 3085–3093.

Büschges, A. (1990). Nonspiking pathways in a joint-control loop of the stick insect carausius morosus. *Journal of Experimental Biology*, *151*, 133–160.

Büschges, A., Kittmann, R., & Schmitz, J. (1994). Identified nonspiking interneurons in leg reflexes and during walking in the stick insect. *Journal of Comparative Physiology A*, *174*(6), 685–700.

Chiel, H. J., Beer, R. D., Quinn, R. D., & Espenschied, K. S. (1992). Robustness of a distributed neural network controller for locomotion in a hexapod robot. *IEEE Transactions on Robotics and Automation*, *8*(3), 293–303.

Cruse, H., Bartling, C., Dreifert, M., Schmitz, J., Brunn, D. E., Dean, J., et al. (1995). Walking: A complex behavior controlled by simple networks. *Adaptive Behavior*, *3*(4), 385–418.

Dewhirst, O. P. (2013). *Validation of nonlinear system identification models of the locust hind limb control system using natural stimulation*. (Ph.D. thesis), UK: Southampton University.

Dewhirst, O. P., Angarita-Jaimes, N., Simpson, D. M., Allen, R., & Newland, P. L. (2012). A system identification analysis of neural adaptation dynamics and nonlinear responses in the local reflex control of locust hind limbs. *Journal of Computational Neuroscience*, 1–20.

Dewhirst, O. P., Simpson, D. M., Allen, R., & Newland, P. L. (2009). Neuromuscular reflex control of limb movement—validating models of the locusts hind leg control system using physiological input signals. In *4th international IEEE/EMBS conference on neural engineering, 2009* (pp. 689–692).

DiCaprio, R. A. (2003). Nonspiking and spiking proprioceptors in the crab: nonlinear analysis of nonspiking TCMRO afferents. *Journal of Neurophysiology*, *89*(4), 1826–1836.

Eiben, A. E., & Smith, J. E. (2003). *Introduction to evolutionary computing*. SpringerVerlag.

Field, L. H., & Burrows, M. (1982). Reflex effects of the femoral chordotonal organ upon leg motor neurones of the locust. *Journal of Fish Biology*, *101*(1), 265–285.

Field, L. H., & Matheson, T. (1998). Chordotonal organs of insects. In P. D. Evans (Ed.), *Advances in insect physiology, Vol. 27* (pp. 1–228). Academic Press.

Gamble, E. R., & DiCaprio, R. A. (2003). Nonspiking and spiking proprioceptors in the crab: White noise analysis of spiking CB-chordotonal organ afferents. *Journal of Neurophysiology*, *89*(4), 1815–1825.

Goldman, M. S., Golowasch, J., Marder, E., & Abbott, L. F. (2001). Global structure, robustness, and modulation of neuronal models. *The Journal of Neuroscience*, *21*(14), 5229–5238.

Haykin, S. (1999). *Neural networks: a comprehensive foundation* (2nd ed.). Prentice Hall PTR.

Horn, D., Ruppin, E., Usher, M., & Herrmann, M. (1993). Neural network modeling of memory deterioration in alzheimer's disease. *Neural Computation*, *5*, 736–749.

Hunt, K. J., Sbarbaro, D., Zbikowski, R., & Gawthrop, P. J. (1992). Neural networks for control systems—A survey. *Automatica*, *28*(6), 1083–1112.

Hunter, I. W., & Korenberg, M. J. (1986). The identification of nonlinear biological systems: Wiener and Hammerstein cascade models. *Biological Cybernetics*, *55*, 135–144.

Jain, A. K., Jianchang, M., & Mohiuddin, K. M. (1996). Artificial neural networks: a tutorial. *Computer*, *29*(3), 31–44.

Kennedy, J., & Eberhart, R. (1995). Particle swarm optimization. In *IEEE international conference on neural networks. proceedings. Vol. 4, 1944* (pp. 1942–1948).

Kondoh, Y., Okuma, J., & Newland, P. L. (1995). Dynamics of neurons controlling movements of a locust hind leg: Wiener kernel analysis of the responses of proprioceptive afferents. *Journal of Neurophysiology*, *73*(5), 1829–1842.

Korenberg, M. J., & Hunter, I. W. (1986). The identification of nonlinear biological-systems—LNL cascade models. *Biological Cybernetics*, *55*, 125–134.

Marder, E., & Taylor, A. L. (2011). Multiple models to capture the variability in biological neurons and networks. *Nature Neuroscience*, *14*(2), 133–138.

Marmarelis, P. V. Z. (2004). *Nonlinear dynamic modeling of physiological systems*. Wiley.

Marmarelis, P. Z., & Naka, K. (1972). White-noise analysis of a neuron chain: an application of the Wiener theory. *Science*, *175*(4027), 1276–1278.

Marmarelis, P. Z., & Naka, K. I. (1973a). Nonlinear analysis and synthesis of receptive-field responses in the catfish retina. I. Horizontal cell leads to ganglion cell chain. *Journal of Neurophysiology*, *36*(4), 605–618.

Marmarelis, P. Z., & Naka, K. I. (1973b). Nonlinear analysis and synthesis of receptive-field responses in the catfish retina. II. One-input white-noise analysis. *Journal of Neurophysiology*, *36*(4), 619–633.

Newland, P. L., & Kondoh, Y. (1997). Dynamics of neurons controlling movements of a locust hind leg III. Extensor tibiae motor neurons. *Journal of Neurophysiology*, *77*(6), 3297–3310.

Palm, G., & Poggio, T. (1977). Wiener-like system identification in physiology. *Journal of Mathematical Biology*, *4*(4), 375–381.

Sarkar, A. X., Christini, D. J., & Sobie, E. A. (2012). Exploiting mathematical models to illuminate electrophysiological variability between individuals. *Journal of Physiology-London*, *590*(11), 2555–2567.

Schneidman, E., Brenner, N., Tishby, N., van Steveninck, R. R., & Bialek, W. (2001). Universality and individuality in a neural code. *NIPS*, *13*, 159–165.

Shi, Y., & Eberhart, R. C. A (1998a). Modified particle swarm optimizer. In *The 1998 IEEE international conference on evolutionary computation proceedings. IEEE world congress on computational intelligence* (pp. 69–73).

Shi, Y., & Eberhart, R. C. (1998b). Parameter selection in particle swarm optimization. In *Evolutionary programming VII* (pp. 591–600). Springer.

Suraweera, N. P., & Ranasinghe, D. N. A (2008). Natural algorithmic approach to the structural optimisation of neural networks. In *4th international conference on information and automation for sustainability* (pp. 150–156).

Tötterman, S., & Toivonen, H. T. (2009). Support vector method for identification of Wiener models. *Journal of Process Control*, *19*(7), 1174–1181.

Twickel, A., Büschges, A., & Pasemann, F. (2011). Deriving neural network controllers from neuro-biological data: implementation of a single-leg stick insect controller. *Biological Cybernetics*, *104*(1–2), 95–119.

Waibel, A., Hanazawa, T., Hinton, G., Shikano, K., & Lang, K. J. (1989). Phoneme recognition using time-delay neural networks. *IEEE Transactions on Acoustics, Speech and Signal Processing*, *37*(3), 328–339.

Webb, A. R., Lowe, D., & Bedworth, M. D. (1988). A comparison of nonlinear optimisation strategies for feed-forward adaptive layered networks. DTIC Document.

White, H. (1988). Economic prediction using neural networks: the case of IBM daily stock returns. In *IEEE international conference on neural networks, Vol. 452* (pp. 451–458).

Xing, L., & Pham, D. T. (1995). *Neural networks for identification, prediction, and control*. Springer-Verlag New York, Inc.